Lab report
E213 Analysis of Z^0 Decay

Chenhuan Wang and Harilal Bhattarai

October 1, 2020

This is abstract.

1. Introduction

This is introduction.

2. Theory

Decay width The partial decay width of Z^0 decay into fermion f is

$$\Gamma_f = \frac{\sqrt{2}N_c^f}{12\pi} G_F M_Z^3 \left((g_V^f)^2 + (g_A^f)^2 \right) \tag{1}$$

with

$$g_V^f = I_3^f - 2Q_f \sin^2\theta_W$$
$$g_A^f = I_3^f$$

One needs to be aware that Γ_f contains contribution from both chiralities, and I_3 here refers to only the weak isospin of left-handed fermions (by definition right handed fermions have no weak isospin).

Partial cross section of $Z^0 \to f\bar{f}$ is given by [1]

$$\sigma_f(s) = \frac{12\pi}{M_Z^2} \frac{s\Gamma_e\Gamma_f}{(s-M_Z^2)^2 + (s^2\Gamma_Z^2/M_Z^2)} \tag{2}$$

Angular distribution In $ee \to ee$ scattering, two relevant channels have different angular dependences. For s-channel,

$$\frac{\mathrm{d}\sigma}{\mathrm{d}\Omega}_s \sim (1+\cos^2\Theta) \tag{3}$$

For t-channel,

$$\frac{\mathrm{d}\sigma}{\mathrm{d}\Omega}_t \sim (1-\cos^2\Theta)^{-2} \tag{4}$$

Forward-Backward Asymmetry near Z^0 resonance can be approximated by

$$\begin{aligned} A_{\mathrm{FB}}^f &\approx \frac{-3}{2} \frac{a_e a_f Q_f \,\mathrm{Re}(\chi)}{(v_e^2+a_e^2)(v_f^2+a_f^2)} \\ &= \frac{-3}{2} \frac{a_e a_f Q_f}{(v_e^2+a_e^2)(v_f^2+a_f^2)} \frac{s(s-M_Z^2)}{(s-M_Z^2)^2+(s\Gamma_Z/M_Z)^2} \end{aligned} \tag{5}$$

3. Pre-lab tasks

Using equation (1), one finds

$$\Gamma_e = \Gamma_\mu = \Gamma_\tau = 83.40\,\mathrm{MeV} \tag{6}$$

The decay widths to leptons of three generations are the same because of lepton universality and neglecting the masses. With the same equation, decay width to quarks in total is

$$\begin{aligned} \Gamma_u = \Gamma_c &= 285.34\,\mathrm{MeV} \\ \Gamma_d = \Gamma_s = \Gamma_b &= 367.79\,\mathrm{MeV} \end{aligned}$$

It is significantly larger, since there are more quarks in SM and quarks carry more degrees of freedom (color) than leptons. Decays to neutrinos are invisible for detector in LEP, but still they have the width of

$$\Gamma_\nu = 165.84\,\mathrm{MeV} \tag{7}$$

Hadronic part

$$\Gamma_{\mathrm{h}} = \sum_{\forall q \neq t} \Gamma_q = 1674.06\,\mathrm{MeV} \tag{8}$$

Charged decay

$$\Gamma_{\mathrm{charged}} = 3\Gamma_e = 250.17\,\mathrm{MeV} \tag{9}$$

Invisible decay

$$\Gamma_{\mathrm{inv}} = 3\Gamma_\nu = 497.52\,\mathrm{MeV} \tag{10}$$

In total (except unknown decays)

$$\Gamma_{\mathrm{total}} = 3\Gamma_e + \Gamma_h + 3\Gamma_\nu = 2421.75\,\mathrm{MeV} \tag{11}$$

decay type	partial width/MeV	partial cross section/10^{-5}MeV^{-2}
hadronic	1674.06	10.79
charged	250.17	1.61
invisible	497.52	3.21
total	2421.75	15.61

Table 1: Decays widths and partial cross sections

Assume that there is another generation of light fermions, the total width of Z^0 would be

$$\Gamma'_{\mathrm{total}} = \Gamma_{\mathrm{total}} + \Gamma_e + \Gamma_\nu + \Gamma_u + \Gamma_d = 3324.11\,\mathrm{MeV} \tag{12}$$

It would be a change of 37% percent!

The differential cross section $\frac{d\sigma}{d\Omega}$ has different angular dependencies for s- and t-channels, see equations (3) and (4). Simply plotting without the proportional constant in front shows where s- or t-channels dominates the process, see figure. 1. At small angles, t-channel dominates,

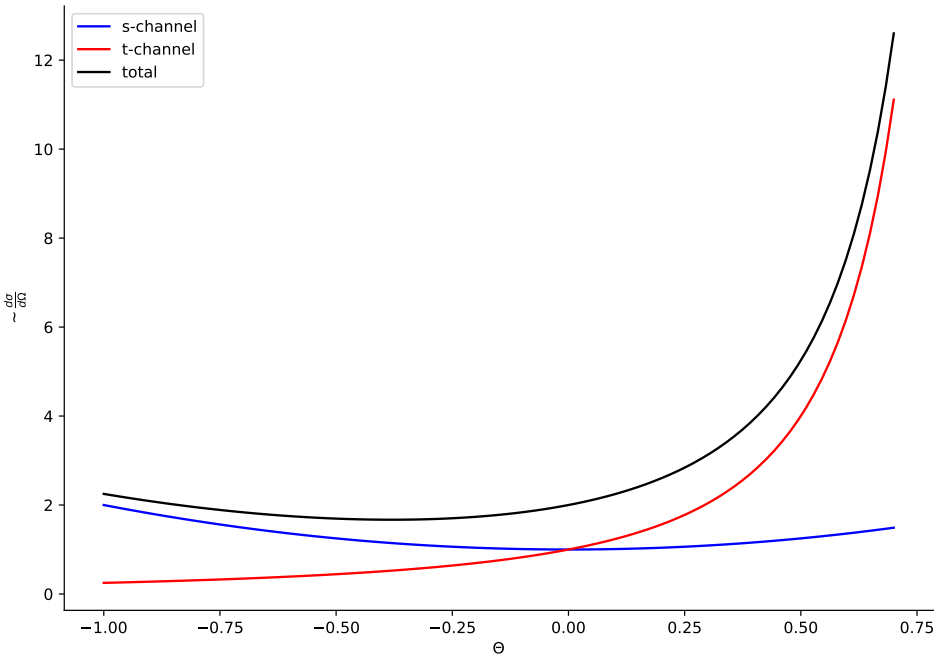

Figure 1: Angular dependencies of two channels.

whereas at large angles, s-channel dominates.

Energy[GeV] $/\sin^2(\theta_W)$	0.21	0.23	0.25
89.225	−0.0379	−0.0420	−0.0451
91.225	−0.0386	−0.0428	−0.0459
93.225	−0.0394	−0.0436	−0.0468

4. Event display

5. Statistical Analysis

Mode selection With large datasets, previous "event display" method will no longer be efficient and accurate. Thus data analysis tools are necessary. Here `root` is used and three macros to apply cuts are already implemented. As before we have four sets of Monte Carlo simulated data in order to find the optimal cuts, then there are a couple of real data samples.

First of all, there are a couple of general cuts. The collider energy of LEP is $\sim 200\,\text{GeV}$. Thus the scalar sum of momenta should be maximally around this value. Events with even larger momenta are caused by various unphysical processes. Secondly, the data here is written such as when there are multiple outgoing positive particles, `cos_thet` $= 1000$. For ee and $\mu\mu$ process, it should not be possible, since no hadronisation can occur and initial/final state radiation for these two only involve photons. So for these two event selections, cut `cos_thet` $<= 1.0$ is applied, see figure 2. After the cut(s), there are 56613 ee events, 89646 $\mu\mu$ events, 79099 $\tau\tau$ events, and 98100 qq events.

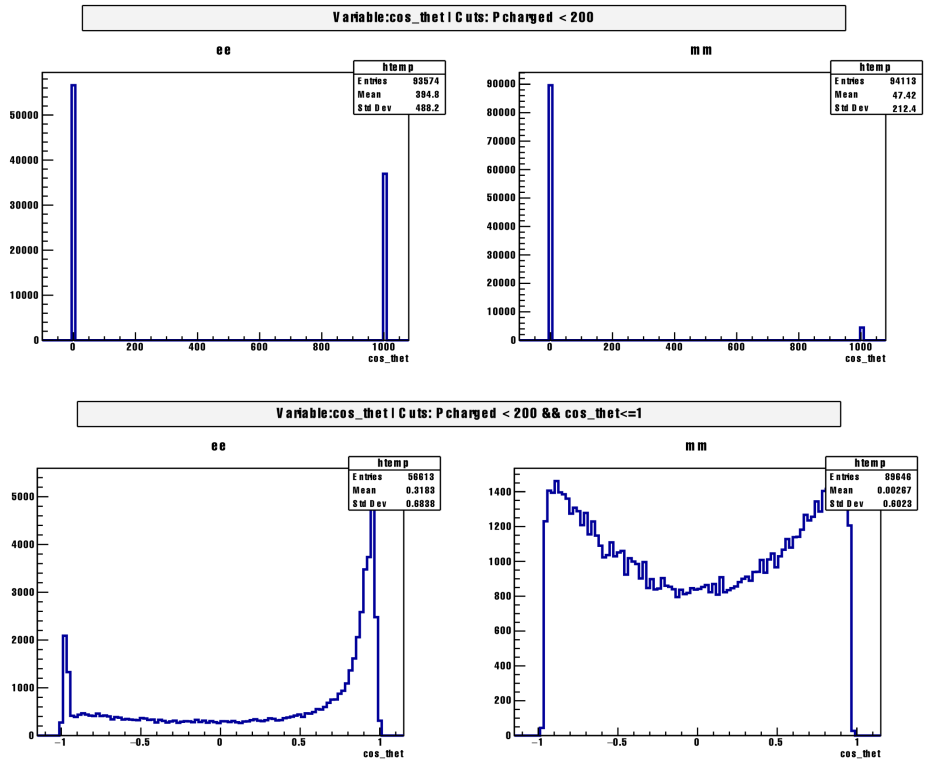

Figure 2: Distribution of `cos_thet` before and after `cos_thet` cut.

In event display part, we had success using cut `Ncharged` > 7 for qq processes. We conclude that this is no longer sufficient, since there are quite many $\tau\tau$ contamination, see figure 3. While roughly 5% percent of qq events are lost, $\tau\tau$ events are barely present and ee, $\mu\mu$ are completely cut. So the 5% percent are considered as acceptable "casualties". After the cut for qq, no ee or $\mu\mu$ are left, 78 $\tau\tau$ survives and 92688 qq events remain.

Follow the same receipt as in event display part, we try to separate ee events from other leptonic channels. Cut in number of charged track remains the same: `Ncharged` < 4 or (≤ 3). Same as before `E_ecal` of ee events have peak at around 80 GeV. `E_ecal` cut is changed to `E_ecal` > 60, since there is virtually no events even at `E_ecal` $= 60$, see figure 4. `E_hcal` cut is similar to before, just relaxed a little bit (to `E_hcal < 2`), since some of events have higher `E_hcal` as previous cut, see figure 5. In the end, we end up with 51679 ee events, 0 $\mu\mu$, 910 $\tau\tau$ events, and 1 qq event.

For $\mu\mu$ selection, cut in `Ncharged` is the same as ee: `Ncharged < 4`. We have already seen in figure 4 that `E_ecal` of $\mu\mu$ has a peak around 0, so the `E_ecal` cut for ee gets inverted as cut for $\mu\mu$: `E_ecal` < 60. Then remaining $\tau\tau$ events can be excluded with the help of `Pcharged`, see figure 6. ee and qq events are basically cut away, only unwanted events are $\tau\tau$. `Pcharged` distributions of $\mu\mu$ and $\tau\tau$ are separated quite nicely, although some $\mu\mu$ events have `Pcharged` ≈ 0. A cut at `Pcharged` > 70 will remove most of $\tau\tau$ events while preserve most of $\mu\mu$ events. After combinations of these cuts, 144 ee events, 83228 $\mu\mu$ events, 480 $\tau\tau$ events and zero qq event survive.

$\tau\tau$ can be picked out using the same cuts for $\mu\mu$ expect `Pcharged` cut gets inverted. Since there is a small peak at `Pcharged` $= 0$ in ee and $\mu\mu$ events, see figure 6, a lower bound in `Pcharged` should be set as well. Thus for $\mu\mu$: $1 <$ `Pcharged` < 60. E_ecal cut should be adjusted a bit. In figure 4, there are still quite substantial amount of $\tau\tau$ event between $60 <$ `E_ecal` < 70. Thus we have for $\tau\tau$: `E_ecal` < 70. Cut in `Ncharged` is relaxed to < 5 for better efficiency. After all these cuts, we have 243 ee events, 1446 $\mu\mu$ events, 66990 $\tau\tau$ events, and 38 qq events.

All the cuts are summarizes in table 2

mode	`cos_thet`	`Pcharged`	`Ncharged`	`E_ecal`	`E_hcal`
ee	≤ 1	< 200	< 4	> 60	< 2
$\mu\mu$	≤ 1	$> 70, < 200$	< 4	< 60	
$\tau\tau$		$> 1, < 60$	< 5	< 70	
qq		< 200	> 10		

Table 2: All cuts applied to select decay modes

Channel selection

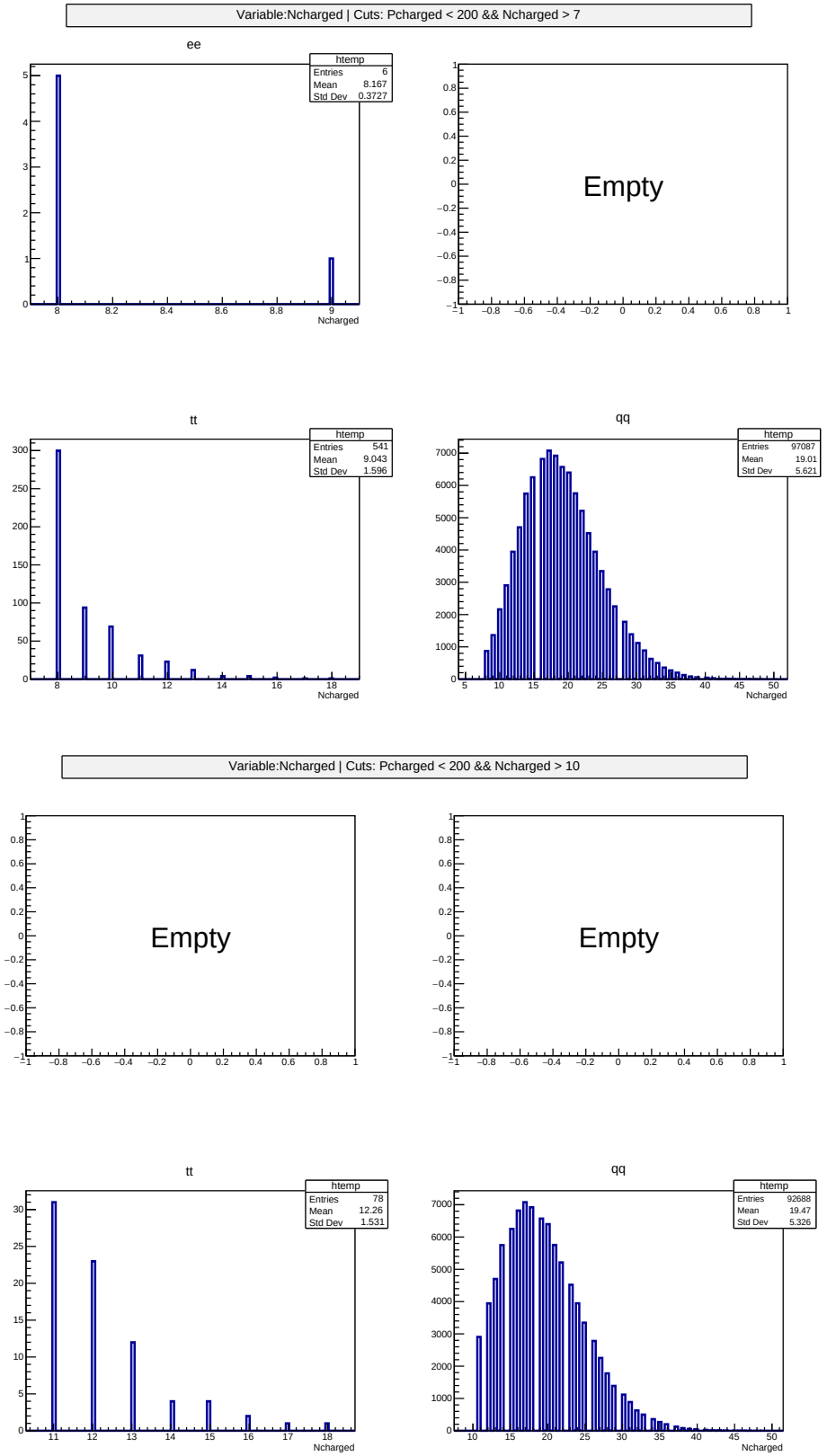

Figure 3: Number of charged tracks (`Ncharge`) before and after the refined cut for qq events.

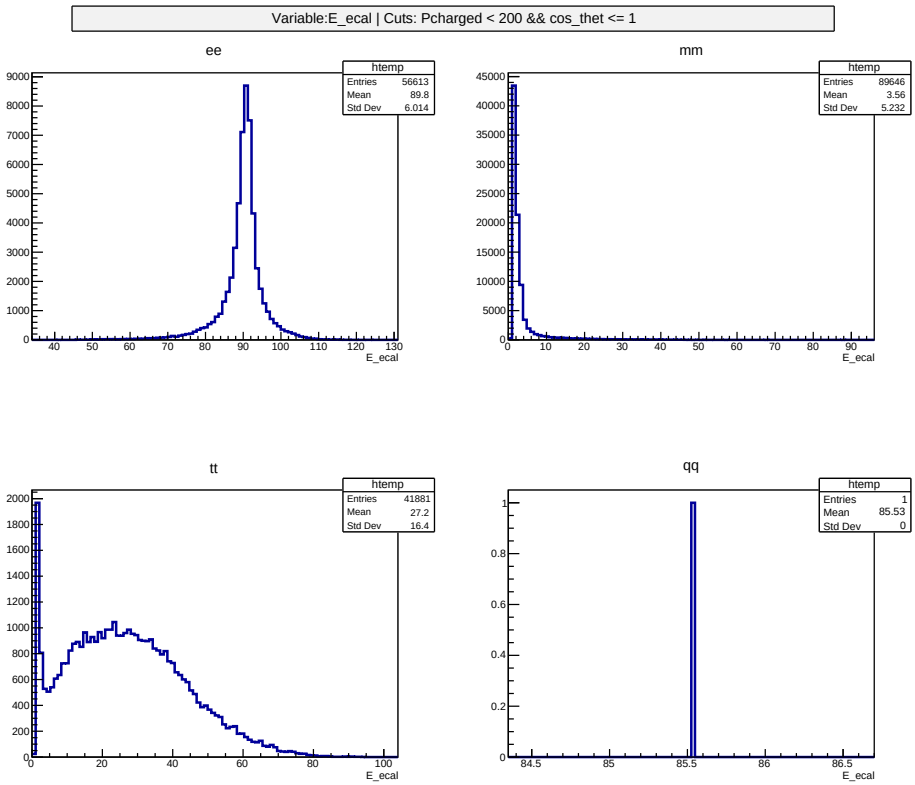

Figure 4: `E_ecal` distribution before `E_ecal` cut for ee.

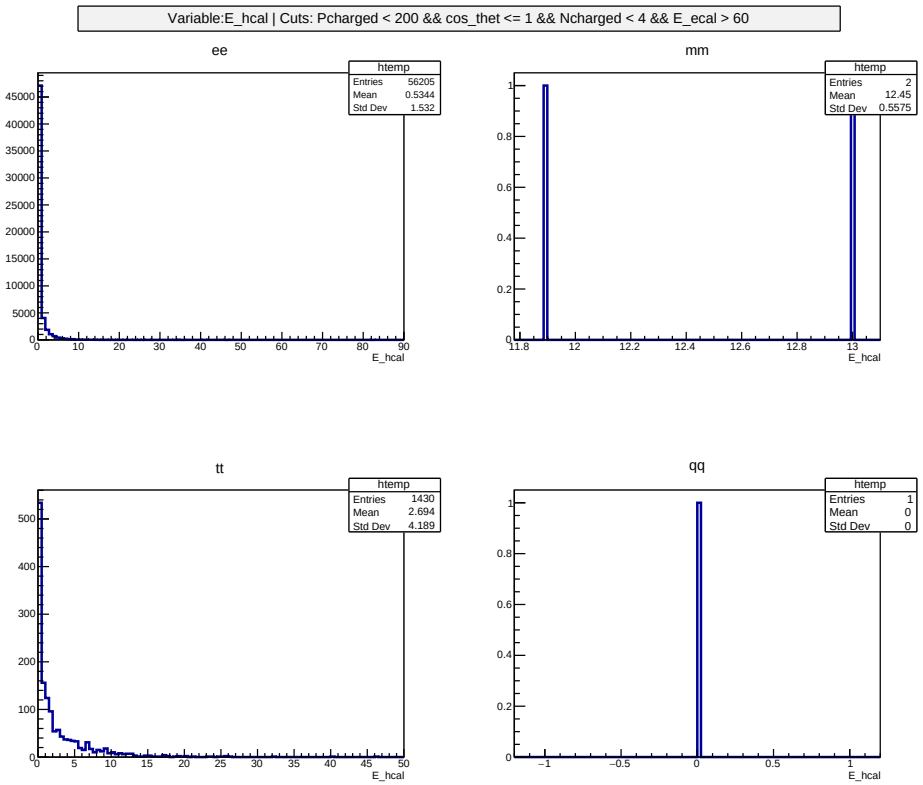

Figure 5: `E_hcal` distribution after `E_ecal` but before `E_hcal` cut for ee.

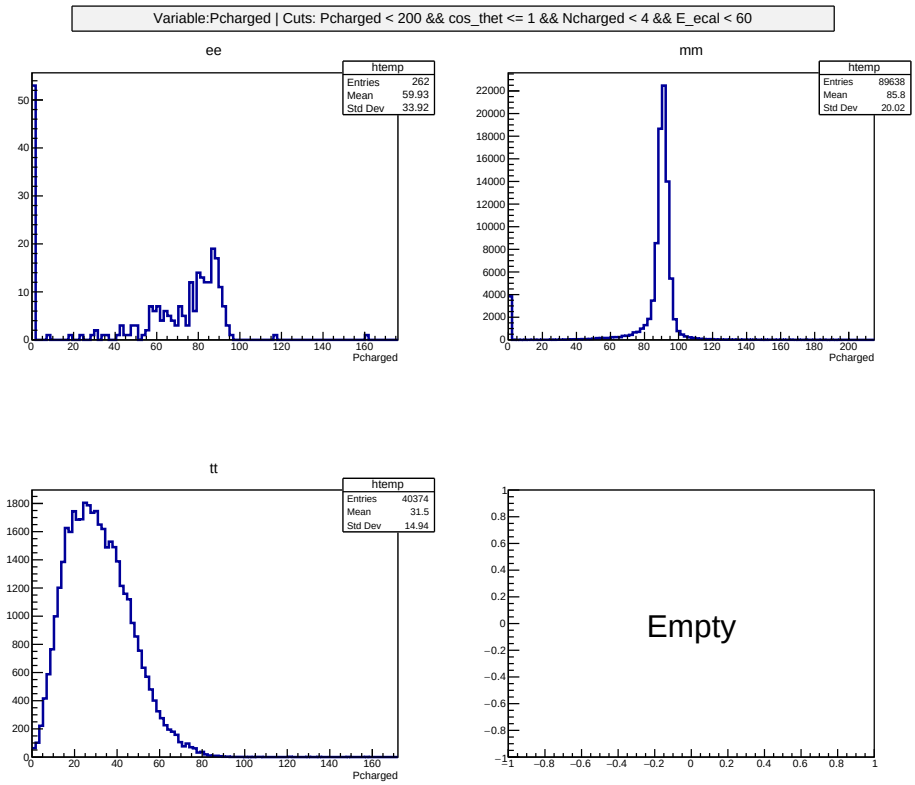

Figure 6: `Pcharged` distribution after `E_ecal` cut for $\mu\mu$.

6. Conclusion and outlook

A. Appendix

A.1. Table for Question 5.6

Event	Ctrk(N)	Ctrk(Sump)	Ecal(SumE)	Hcal(SumE)	Comment
1	2	50.9	82.6	0.0	
2	2	91.0	90.0	0.0	
3	3	82.5	92.3	0.0	
4	2	80.9	86.8	0.0	
5	2	38.1	89.5	0.0	
6	2	83.8	87.5	0.0	
7	2	87.4	93.2	0.0	
8	2	69.3	90.7	0.0	
9	2	86.1	89.4	0.5	
10	2	90.3	90.6	0.0	
11	2	92.1	88.5	0.4	
12	3	81.7	91.6	0.0	
13	2	89.6	92.5	0.0	
14	2	61.1	89.2	0.0	
15	3	88.4	89.1	0.0	
16	2	90.9	90.5	0.3	
17	2	64.6	88.8	0.0	
18	2	95.6	96.2	0.0	
19	2	93.0	90.8	0.0	
20	2	94.1	89.2	0.0	

Table 3: caption

A.2. 5.10

$\sqrt{s}$	cuts	number of events
88.47		6194
88.47	ee	125
88.47	mm	136
88.47	tt	157
88.47	qq	3359
89.47		7861
89.47	ee	198
89.47	mm	233
89.47	tt	207
89.47	qq	5036
90.22		9779
90.22	ee	223
90.22	mm	329
90.22	tt	249
90.22	qq	7157
91.22		114 394
91.22	ee	2313
91.22	mm	3761
91.22	tt	3247
91.22	qq	87 844
91.97		18 931
91.97	ee	346
91.97	mm	664
91.97	tt	538
91.97	qq	14 571
92.96		8599
92.96	ee	139
92.96	mm	257
92.96	tt	248
92.96	qq	6303
93.71		10 125
93.71	ee	191
93.71	mm	318
93.71	tt	281
93.71	qq	7029

Table 4: Raw data for partial cross section

References

[1] Unknown. *E213 Analysis of Z0 Decay.*